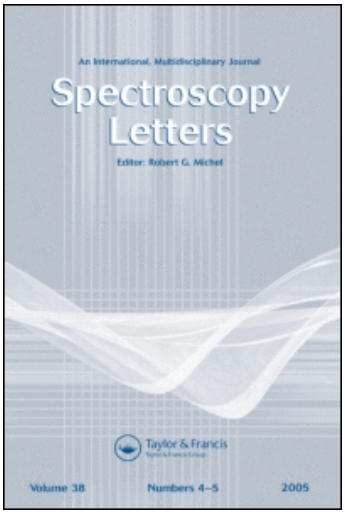

Spectroscopy Letters

Publication details, including instructions for authors and subscription information:
http://www.informaworld.com/smpp/title~content=t713597299

Interpretation of FTIR Spectra by Principal Components-Artificial Neural Networks

Bingping Liu[ab]; Yan Li[a]; Lin Zhang[a]; Junde Wang[a]
[a] Laboratory of Advanced Spectroscopy, Nanjing University of Science & Technology, Nanjing, People's Republic of China [b] Department of Chemistry, Qufu Normal University, Qufu, People's Republic of China

To cite this Article Liu, Bingping , Li, Yan , Zhang, Lin and Wang, Junde(2006) 'Interpretation of FTIR Spectra by Principal Components-Artificial Neural Networks', Spectroscopy Letters, 39: 4, 373 — 385
To link to this Article: DOI: 10.1080/00387010600803664
URL: http://dx.doi.org/10.1080/00387010600803664

Spectroscopy Letters, 39: 373–385, 2006

ISSN 0038-7010 print/1532-2289 online
DOI: 10.1080/00387010600803664

Interpretation of FTIR Spectra by Principal Components–Artificial Neural Networks

Bingping Liu
Laboratory of Advanced Spectroscopy, Nanjing University of Science & Technology, Nanjing, People's Republic of China and Department of Chemistry, Qufu Normal University, Qufu, People's Republic of China

Yan Li, Lin Zhang, and Junde Wang
Laboratory of Advanced Spectroscopy, Nanjing University of Science & Technology, Nanjing, People's Republic of China

Abstract: In order to improve the training speed and increase the predictive ability of artificial neural networks, principal component analysis (PCA) and partial least squares (PLS) were introduced to compress the original data. The principal components (PCs) of FTIR spectroscopic data matrix were obtained by PCA and PLS methods respectively, which were used as the inputs of neural networks. Results indicated that improvement was achieved in three aspects when the PCs instead of the original data were input to the networks. First, iterations were distinctly decreased from 8000 to less than 10. Second, computation time was shortened from 34.95 s to less than 1 s. Third, standard error of prediction (%SEP), mean relative error (MRE), and the root mean square error of prediction (RMSEP) decreased by 35% for the singular value decomposition–artificial neural network (SVD-ANN) and 80% for the nonlinear iterative partial least squares–ANN (NIPALS-ANN) or so, which means that the predictive ability was improved significantly. In addition, F-test was introduced to compare the performance of PCA and PLS for compression of original data, and it was shown that the latter model was more efficient. The presented methodologies of variable selection provide a simple and rapid technique for ANN to interpret FTIR spectra accurately and are advantageous to the widespread use of artificial neural networks.

Keywords: Artificial neural network, FTIR, multicomponent analysis, partial least squares, principal component analysis, selection of variables

Received 16 April 2005, Accepted 15 May 2006
Address correspondence to Yan Li, Laboratory of Advanced Spectroscopy, Nanjing University of Science & Technology, Nanjing 210014, People's Republic of China. E-mail: yanli@mail.njust.edu.cn

INTRODUCTION

Artificial neural networks are mathematical models of biological neural systems. Over the past few years, the artificial neural network (ANN) modeling technique has attracted an increasing interest as a very promising method in many aspects, such as nonlinear calibration,[1–5] quantitative structure–activity relationship,[6,7] optimization of experimental conditions,[8] and modeling of kinetic data.[9,10] However, there must be a lot of training sets to train the network, which makes the structure of the networks very complex and causes the predictive ability to be depressed, especially for the spectroscopic data. After the measurement was made with spectrometer, hundreds and thousands of variables were collected from each spectrum. If all the data are input to the neural network, the matrix of training sets is so large that the number of iterations is too, much and it's burdensome for the microcomputer to finish such complex calculations. The information with noises or interfering signals is also introduced to the model, which actually deteriorates the accuracy and/or precision of the neural networks. In other way, there is a large correlation to some chosen features, which makes it easy to be overfitted. If only several data at different wavenumbers are used, the information of the whole spectrum will not be fully included, and it's possible to lose part of the features. In these cases, it's very necessary to select some representative data to train the network.

The earliest method to select the variables is stepwise regression analysis (SRA). It chooses the variables based on the output of systems, but the selected data have relativity, and the results depend on the sequence of training samples. Thus it's difficult to find a model with best prediction ability. In recent years, genetic algorithm (GA), which selects a subset of variables, has been widely used.[11–14] Studies have shown that GA performs equivalently or even better compared with the traditional methods with less than 30 dimensions.[15] For higher dimension problems, however, the performance seems to degrade.

Instead of selecting a subset of the available features, principal component analysis (PCA)[16–18] and partial least squares (PLS),[19] which are linear combinations of all available features, were introduced in this paper to reduce the dimensionality. To each FTIR spectrum, 82 variables were obtained from 1272 to 624 cm^{-1} in 8 cm^{-1} intervals. Then the principal components of the data matrix were extracted by PCA and PLS respectively, which were used as the inputs of the new networks. After the original data were processed, it was found that iterations and computation time were obviously decreased, and the prediction ability of the networks was significantly improved. In the research, a comparison between the singular value decomposition–artificial neural network (SVD-ANN) and the nonlinear iterative partial least squares–ANN (NIPALS-ANN) models was made. Results indicated that PLS model was better to select the principal components than PCA model.

THEORETICAL

PCA and PLS

PCA and PLS are two multivariate full-spectrum calibration techniques that have received considerable attention. Many researchers have observed that inclusion of extra principal components or latent variables in the calibration model can express nonlinear responses.[20,21] Both methods consider the information of all the available features and then condense them into new variables that are orthogonal and span the multidimensional space of X, which is the $(n \times m)$ matrix of n calibration spectra measured at m different wavenumbers. The new variables are linear combinations of the original data and are calculated in order of importance, so by keeping only the first few variables, a noise reduction can be achieved, and at the same time, they express the structure and the character of the old variables as much as possible.

In PCA model, the principal components (PCs) were obtained by the singular value decomposition procedure (SVD).

$$X = UWV^T \tag{1}$$

where U and V are the orthonormal matrices spanning the respective row and column spaces of the data matrix (X). W is a diagonal matrix whose elements are the square root of the eigenvalues. The eigenvectors included in U are named as PCs, which were used as inputs to ANN model (SVD-ANN). For "unknown" samples, the PCs are computed by the equation below:

$$U_{\text{unknown}} = X_{\text{unknown}} VW^{-1} \tag{2}$$

where X_{unknown} is the unknown sample's measured spectrum. U_{unknown} is the unknown sample's vector of new orthogonal variables.

In PLS modeling, nonlinear iterative partial least squares (NIPALS) was used to calculate PLS model parameters. When calculating the new variables, both matrix X and Y are used. Here, matrix Y stands for the concentrations of J components for I samples. The PCs are calculated in order of importance by maximizing the covariance between Y and linear combinations of the x-variables. The linear regression equation can be written as

$$X = TP^T + F = \sum_{i=1}^{d} t_i p_i^T + F \tag{3}$$

$$Y = UQ^T + E = \sum_{i=1}^{d} u_i q_i^T + E \tag{4}$$

where T and U are the score matrices of X and Y. P and Q are their loading matrices. F and E are the matrices of the residual spectra. d is the number

of PCs, which was determined on the basis of cross-validation method. Then a linear relationship is established between T and U.

$$U = TB \tag{5}$$

where B is the matrix of regression vectors. In this model, the score matrix T is the new input of ANN model (NIPALS-ANN).

ANN Modeling

Three layers back-propagation networks were employed in this study. The detailed description of its theory has been given in other references.[22–26] In our models, the input signals are absorbance values, and the outputs are the concentrations of the compounds. The number of neurons in the hidden layer and the number of iterations were determined by the trial-and-error method. During the learning process, the weights of hidden and output layers were adjusted by back-propagation algorithm. In this work, the optimum network was determined by the degree of approximation,[27] and the training process was terminated when the errors reached the minimum.

Definition of %SEP, MRE, RMSEP, and F-Test

The formulas of standard error of prediction (%SEP), mean relative error (MRE), F-test, and the root-mean-square error of prediction (RMSEP) are calculated by Eqs. (6), (7), (8), and (9), respectively. For the calculation of F-test, a confidence level of 95% was set.

$$\%SEP_j = \frac{100}{\bar{c}_j}\left[\frac{\sum_{i=1}^{N}(\hat{c}_{ij} - c_{ij})^2}{N}\right]^{1/2} \tag{6}$$

$$MRE_j = \frac{100}{N}\frac{\sum_{i=1}^{N}|\hat{c}_{ij} - c_{ij}|}{c_{ij}} \tag{7}$$

$$F = \left(\frac{\%SEP_i}{\%SEP_j}\right)^2 \tag{8}$$

$$RMSEP = \sqrt{\frac{\sum_{i=1}^{N}(\hat{c}_{ij} - c_{ij})^2}{N}} \tag{9}$$

where $\hat{c}_{ij}$ is the measured concentration of the jth component for the ith sample, c_{ij} is the real concentration, $\hat{c}_j$ is the mean concentration of the jth component, N is the number of predicted samples, $\%SEP_i$ and $\%SEP_j$ are %SEP of the ith model and the jth model.

MATERIALS AND METHODS

Calibration and Prediction Samples

The database of vapor-phase FTIR spectra used in this paper was from the U.S. Environmental Protection Agency (EPA) library. The air toxic volatile organic compounds (VOCs) aniline, benzene, methanol, toluene, and chloroform, whose spectra are seriously overlapped with each other, were chosen as the analytical objects. The FTIR spectra of these five compounds at 50 ppm are presented in Fig. 1. In this paper, 35 samples and 16 samples were used to train and test the network, respectively. In the samples, there are not any other VOCs except these five compounds.

Hardware and Software

The program of ANN was written in MATLAB 6.5. The "newff" function in the Neural Network Toolbox was used to create the network. The "traingdm" function, which used a fast back-propagation algorithm with momentum and an adaptive learning rate, was applied to train the network. The "sim" function was used to simulate the neural networks in the testing phase. The calculation of PCA and PLS was performed using "PLS Toolbox." All the calculations

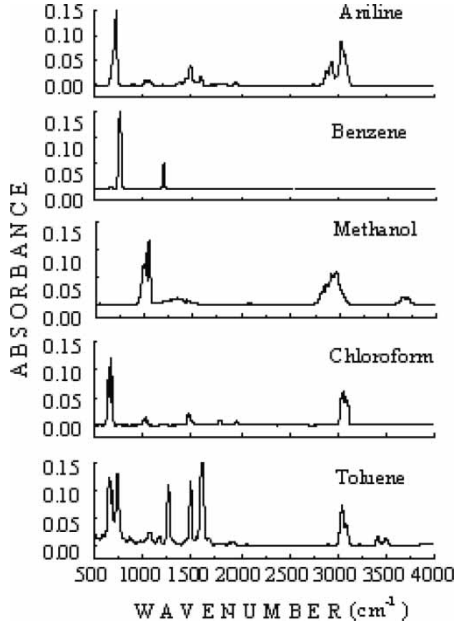

Figure 1. The standard single component spectra of the samples at 50 ppm.

and data processing were carried out in Windows 2000 on a Pentium IV personal computer with 2.4 GHz of CPU and 256 Mbytes of memory.

RESULTS AND DISCUSSION

Parameters of the Optimum Networks and Computation Time

When the input signals were unprocessed, the number of inputs is equal to the number of variables obtained from the spectrum. Based on the peak absorbance of these five compounds, the variables were obtained from 1272 cm^{-1} to 624 cm^{-1} in 8 cm^{-1} intervals, and the total number is 82. When the original data were decomposed by SVD, six PCs were obtained. So the SVD-ANN model had six neurons in the input layer. After the original data were decomposed by NIPALS, the number of PCs was determined according to cross-validation method. In this procedure, the data set is divided into a number of equal-size segments. The NIPALS model is built on all segments except one of them and then is used to estimate variables that are left out of the data. The root mean square error of cross-validation (RMSECV) can be plotted as a function of the number of latent variable number (in Fig. 2). When the number of latent variables (named as PCs) increased from 1 to 5, RMSECV decreased quickly. The reason was that more and more variables with high information description were added to the model. However, when the number of PCs added continuously, RMSECV began to increase slowly. This was caused by the fact that additional latent variables model noise or nonlinearity were added, which worsened the predictive results. So the number of PCs in NIPALS-ANN model was set to be 5.

The number of neurons in hidden layer and the iterations were determined on the basis of the trial-and-error method. These parameters are summarized

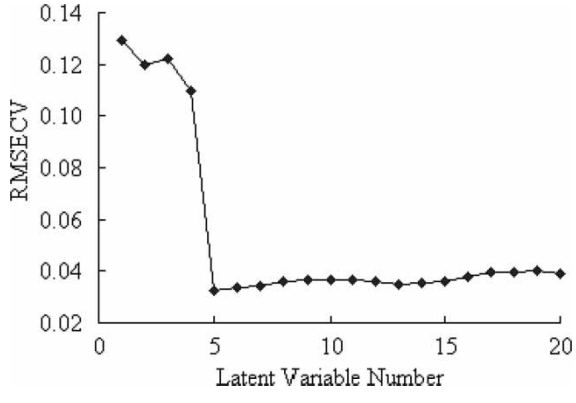

Figure 2. Cross-validation PRESS curve.

in Table 1. From Table 1, it is seen that the structures of these three neural networks were different from each other. After the original data were compressed, the models became much more simple and the number of iterations was obviously decreased from 8000 to 9 for the SVD-ANN model and to 7 for the NIPALS-ANN model. At the same time, computation time was significantly decreased from 34.95 to 0.58 and 0.53 s, respectively.

Prediction of Unknown Samples

Three neural networks were used to interpret 18 unknown FTIR spectra. The predictive results are shown in supporting information (Table 2). It indicated that the measured concentrations were all close to the real concentrations. Based on Table 2, standard error of prediction (%SEP), mean relative error (MRE), root mean square error of prediction (RMSEP), and the relative correlation coefficient (R)[28] of predicted concentrations versus actual concentrations were calculated (Table 3). When the inputs were original data, the errors were higher than the corresponding ones in SVD-ANN and NIPALS-ANN. In ANN model, the lowest errors of %SEP, MRE, and RMSEP were 2.86, 2.02, and 0.21. However, the highest errors were only 2.99, 2.80, 0.22 for SVD-ANN model and 0.92, 0.79, 0.07 for NIPALS-ANN model, respectively. The errors (%SEP, MRE, and RMSEP) decreased by 35% for SVD-ANN and 80% for NIPALS-ANN or so. Therefore, the errors of neural networks established by the PCs were decreased obviously, and the predictive ability was significantly improved. The reason is that there is a large correlation to some features for the original data, which deteriorates the predictive ability. After the original data were compressed by PCA and PLS, the vectors were orthogonal, and the unimportant variables containing noisy information have been eliminated.

After the PCs were input to the neural networks, computation time was shortened and the predictive ability was significantly improved. Table 4 presents the results of the F-test for these three models. It can be seen that the values of NIPALS-ANN are higher than those of SVD-ANN, indicating that there is a significant difference between the values of %SEP, and the performance of NIPALS-ANN is much better than SVD-ANN. It is due to

Table 1. Parameters of ANN and computation time

Model	Neurons of input layer	Neurons of hidden layer	Iterations	Computation time (s)
ANN	82	12	8000	34.95
SVD-ANN	6	5	9	0.58
NIPALS-ANN	5	5	7	0.53

ANN, artificial neural network; SVD, singular value decomposition; NIPALS, nonlinear iterative partial least squares.

Table 2. Prediction results of 18 unknown samples

	Compounds (ppm)																			
	Aniline				Benzene				Methanol				Toluene				Chloroform			
No.	C_{real}	C_{meas1}	C_{meas2}	C_{meas3}	C_{real}	C_{meas1}	C_{meas2}	C_{meas3}	C_{real}	C_{meas1}	C_{meas2}	C_{meas3}	C_{real}	C_{meas1}	C_{meas2}	C_{meas3}	C_{real}	C_{meas1}	C_{meas2}	C_{meas3}
1	6.20	6.57	6.52	6.31	9.50	9.42	9.36	9.53	5.80	5.58	5.61	5.69	8.50	8.37	8.25	8.44	8.00	7.76	7.97	7.93
2	7.50	7.78	7.67	7.58	8.50	9.11	8.32	8.52	9.20	9.24	9.16	9.11	8.00	7.98	7.82	7.95	7.50	7.51	7.56	7.45
3	6.50	6.52	6.57	6.50	6.00	6.60	5.85	6.00	6.00	6.10	5.86	6.00	7.50	6.91	7.27	7.50	9.00	8.94	9.00	9.00
4	8.50	8.21	8.53	8.51	7.50	7.00	7.31	7.50	8.00	8.07	8.01	7.99	9.00	8.96	8.85	9.00	5.50	5.48	5.59	5.49
5	6.00	5.91	6.08	6.00	5.80	5.63	5.60	5.80	6.50	6.39	6.55	6.50	7.00	7.33	6.87	7.00	7.00	7.00	7.12	7.00
6	5.80	5.83	5.93	5.91	9.20	8.65	9.01	9.23	7.60	7.22	7.60	7.49	8.50	8.05	8.34	8.44	7.80	7.33	7.88	7.73
7	9.00	8.88	9.19	8.96	6.00	5.39	5.83	5.99	9.40	9.20	9.35	9.44	9.20	9.09	9.01	9.22	8.00	8.52	8.05	8.02
8	7.80	7.77	8.13	7.83	7.50	7.36	7.36	7.51	6.80	6.59	6.60	6.77	8.20	8.08	7.94	8.19	7.00	6.87	6.96	6.98
9	6.20	6.03	6.22	6.19	5.20	5.35	5.03	5.20	7.60	7.55	7.51	7.61	6.80	6.80	6.40	6.80	8.40	8.55	8.43	8.40
10	8.80	9.10	8.97	8.87	8.20	8.34	8.02	8.22	5.60	5.20	5.57	5.52	5.80	5.54	5.63	5.76	6.50	6.32	6.56	6.45
11	5.60	5.84	5.92	5.74	9.40	8.85	9.26	9.44	8.20	7.98	8.01	8.06	7.40	7.66	7.14	7.33	6.40	6.43	6.36	6.31
12	5.20	4.96	5.26	5.29	7.80	8.20	7.59	7.82	6.20	6.61	6.29	6.11	6.60	7.09	6.49	6.55	7.50	7.66	7.64	7.44
13	7.20	7.17	7.16	7.23	6.80	6.74	6.65	6.81	8.50	8.66	8.37	8.47	7.60	7.67	7.38	7.59	8.00	8.09	8.00	7.98
14	5.60	6.02	5.95	5.66	7.00	7.13	6.87	7.02	9.50	9.14	9.28	9.44	7.40	7.73	7.13	7.37	5.50	5.78	5.45	5.46
15	6.70	6.76	6.79	6.75	8.20	8.39	8.00	8.21	6.00	5.88	6.05	5.95	8.60	8.56	8.47	8.57	6.20	6.11	6.32	6.17
16	7.10	7.17	7.26	7.12	6.50	6.30	6.40	6.51	7.20	6.92	6.87	7.18	6.90	6.87	6.57	6.89	7.30	7.25	7.18	7.29
17	8.50	8.75	8.61	8.51	5.80	5.91	5.60	5.80	8.40	8.55	8.43	8.39	5.60	5.63	5.46	5.59	8.10	8.08	8.20	8.09
18	9.00	8.77	9.23	9.06	9.40	9.15	9.24	9.42	5.40	5.09	5.31	5.34	9.30	9.06	9.10	9.27	6.70	6.56	6.73	6.66

C_{real}, C_{meas1}, C_{meas2}, and C_{meas3} stand for real concentrations and measured concentrations by ANN, SVD-ANN, and NIPALS-ANN, respectively.

Table 3. Statistical parameters calculated for the prediction using ANN, SVD-ANN, and PLS-ANN models

	%SEP			RMSEP			MRE			R		
Compounds	ANN	SVD-ANN	NIPALS-ANN	ANN	SVD-ANN	NIPALS-ANN	ANN	SVD-ANN	NIPALS-ANN	ANN	SVD-ANN	NIPALS-ANN
Aniline	3.07	2.66	0.92	0.22	0.19	0.07	2.64	2.34	0.79	0.9639	0.9900	0.9985
Benzene	4.90	2.32	0.24	0.36	0.17	0.02	4.10	2.32	0.17	0.9132	0.9995	1.0000
Methanol	3.35	1.90	0.92	0.24	0.14	0.07	3.05	1.51	0.74	0.9685	0.9915	0.9985
Toluene	3.46	2.99	0.46	0.26	0.22	0.04	2.64	2.80	0.35	0.9246	0.9941	0.9993
Chloroform	2.86	1.05	0.59	0.21	0.08	0.04	2.02	0.93	0.47	0.9439	0.9937	0.9990

ANN, artificial neural network; SVD, singular value decomposition; NIPALS, nonlinear iterative partial least squares.
%SEP, standard error of prediction; RMSEP, root mean square error of prediction; MRE, mean relative error; R, relative correlation coefficient.

Table 4. Comparison of different ANN models using the F-test

Compounds	SVD-ANN	NIPALS-ANN
Aniline	1.33	11.14
Benzene	4.46	416.84
Methanol	3.11	13.26
Toluene	1.34	56.58
Chloroform	7.42	23.50

ANN, artificial neural network; SVD, singular value decomposition; NIPALS, nonlinear iterative partial least squares.

the fact that PCA can compress thousands of spectral data into several scores and describe the character of spectra, but the compression does not concern the relationship between the input variables and target outputs. Compared with PCA, PLS considers the influence of the target outputs and the PCs obtained can express the relationship between input variables and output variables more accurately. Therefore, the predictive ability of NIPALS-ANN is better than SVD-ANN model, which could also be seen from the plot of predicted concentrations versus actual concentrations in supporting information (Fig. 3). Figures 3a, 3b, and 3c were derived from ANN, SVD-ANN, and NIPALS-ANN models, respectively. The data in Fig. 3b scattered more seriously than those in Fig. 3c, which indicated that the dispersion between measured concentrations and real ones was larger and the predictive ability was worse in Fig. 3b. Thus, we proposed that PLS used to select the PCs is more efficient than PCA model. However, PCA model is simpler and is easy for programming. If it is not rigorous for the precision of results, researchers can choose PCA to compress the data. Otherwise, we can choose PLS model.

CONCLUSIONS

In order to improve the training speed and the accuracy obtained from artificial neural networks, it was necessary to compress the input data into orthogonal variables. In this study, methods to select variables from FTIR spectroscopic data have been examined. The principal components of 82 FTIR spectroscopic data matrix were extracted by PCA and PLS respectively, which were used as the inputs of neural networks. It was found that when the PCs were input to neural networks, iterations were decreased significantly from 8000 to less than 10, computation time was shortened from 34.95 s to less than 1 s and the errors (%SEP, MRE, and RMSEP) decreased by 35% for SVD-ANN and 80% for NIPALS-ANN or so. The results obtained in this study are sufficient to justify that PCA and PLS are good methods to reduce the noise and the

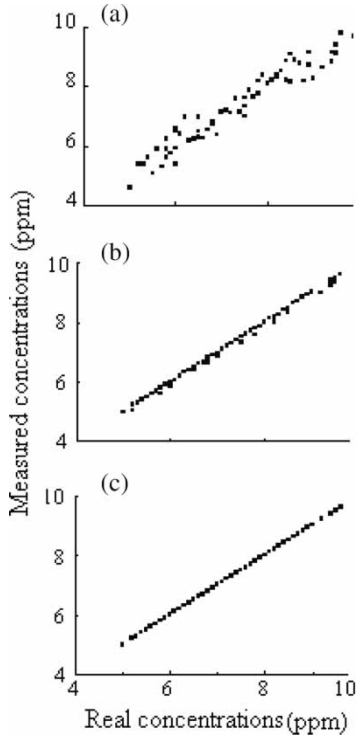

Figure 3. Concentrations of benzene predicted by (a) ANN, (b) SVD-ANN, and (c) NIPALS-ANN against the real concentrations.

dimensions of FTIR spectroscopic data. In addition, the comparison of the values of F-test indicates that PLS is much better than PCA in compressing the data. The presented methodology of variable selection provides a simple but rapid technique for ANN to interpret FTIR spectra accurately, and also urges that artificial neural networks be used widely in analytical chemistry.

In this work, the samples in the validation sets were the same as the training sets. However, when the samples in the validation sets were not included in the training steps, the concentrations of the unknown samples cound not been predicted. In order to solve this problem, further research is being done by our group.

ACKNOWLEDGMENTS

This project was supported by National Natural Science Foundation of China (no. 20175008), China Postdoctoral Science Foundation (2003034386), and Young Scholar Foundation of Nanjing University of Science and Technology (Njust200303).

REFERENCES

1. Martin, M. A.; Santos, J. P.; Agapito, J. A. Application of artificial neural networks to calculate the partial gas concentrations in a mixture. *Sensor Actuat. B* **2001**, *77*, 468–471.
2. Li, Y.; Wang, J. D.; Chen, Z. R.; Zhou, X. T. Artificial neural network for the quantitative analysis of air toxic VOCs. *Anal. Lett.* **2001**, *34* (12), 2203–2219.
3. Li, Y.; Wang, J. D.; Huang, Z. H.; Xu, H. Q.; Zhou, X. T. Monitoring leaking gases by OP-FTIR remote sensing. *J. Environ. Sci. Health A* **2002**, *A37*, 1453–1462.
4. Srivastava, A. K. Detection of volatile organic compounds (VOCs) using SnO_2 gas-sensor array and artificial neural network. *Sensor Actuat. B* **2003**, *96*, 24–37.
5. Dou, Y.; Sun, Y.; Ren, Y. Q.; Ren, Y. L. Artificial neural network for simultaneous determination of two components of compound paracetamol and diphenhydramine hydrochloride powder on NIR spectroscopy. *Anal. Chim. Acta* **2005**, *528*, 55–61.
6. Vaananen, T.; Koskela, H.; Hiltunen, Y.; Ala-Korpela, M. Application of quantitative artificial neural network analysis to 2D NMR spectra of hydrocarbon mixtures. *J. Chem. Inf. Sci.* **2002**, *42*, 1343–1346.
7. Hemmateenejad, B.; Akhond, M.; Miri, R.; Shamsipur, M. Genetic algorithm applied to the selection of factors in principal component-artificial neural networks: application to QSAR study of calcium channel antagonist activity of 1,4-dihydropyridines (nifedipine analogous). *J. Chem. Inf. Sci.* **2003**, *43*, 1328–1334.
8. Guo, W.; Zhu, P.; Brodowsky, H. The study for optimization of chromatographic condition by means of artificial neural networks. *Talanta* **1997**, *44*, 1995–2001.
9. Safavi, A.; Absalan, G.; Maesum, S. Simultaneous determination of V(IV) and Fe(II) as catalyst kinetic run. *Anal. Chim. Acta* **2001**, *432*, 229–233.
10. Wang, C.; Chen, F.; He, X. W. Kinetic detection of benzene/chloroform and toluene/chloroform vapors using a single quartz piezoelectric crystal coated with calix[6]arene. *Anal. Chim. Acta* **2002**, *464*, 57–64.
11. Ding, Q.; Small, G. W.; Arnold, M. A. Genetic algorithm-based wavelength selection for the near-infrared determination of glucose in biological matrixes: initialization strategies and effects of spectral resolution. *Anal. Chem.* **1998**, *70*, 4472–4479.
12. Depczynski, U.; Frost, V. J.; Molt, K. Genetic algorithms applied to the selection of factors in principal component regression. *Anal. Chim. Acta* **2000**, *420*, 217–227.
13. Aleixandre, M.; Sayago, I.; Horrillo, M. C.; Fernandez, M. J.; Ares, L.; Garcia, M.; Santos, J. P.; Gutierrez, J. Analysis of neural networks and analysis of feature selection with genetic algorithm to discriminate among pollutant gas. *Sensor Actuat. B* **2004**, *103*, 122–128.
14. Gestal, M.; Gomez-Carracedo, M. P.; Andrade, J. M.; Dorado, J.; Fernandez, E.; Prada, D.; Pazos, A. Classification of apple beverages using artificial neural networks with previous variable selection. *Anal. Chim. Acta* **2004**, *524*, 225–234.
15. Jain, A.; Zongker, D. Feature selection: evaluation, application and small sample performance. *IEEE Trans. Pattern Anal. Machine Intell.* **1997**, *19*, 153–158.
16. Safavi, A.; Abdollahi, H.; Hormozi Nezhad, M. R. Artificial neural networks for simultaneous spectrophotometric differential kinetic determination of Co(II) and V(IV). *Talanta* **2003**, *59*, 515–523.
17. Penza, M.; Cassano, G. Application of principal component analysis and artificial neural networks to recognize the individual VOCs of methanol1/2-propanol in a binary mixture by SAW multi-sensor array. *Sensor Actuat. B* **2003**, *89*, 269–284.

18. Dorn, E. D.; McDonald, G. D.; Storrie-Lombardi, M. C.; Nealson, K. H. Principal component analysis and neural networks for detection of amino acid biosignatures. *Icarus* **2003**, *166*, 403–409.
19. Shamsipur, M.; Hemmateenejad, B.; Akhond, M. Multicomponent acid–base titration by principal component-artificial neural network calibration. *Anal. Chim. Acta* **2002**, *461*, 147–153.
20. Li, Y.; Yang, S. L.; Wang, J. D.; Gu, B. H.; Liu, F. Simultaneous determination of multicomponents in air toxic organic compounds using artificial neural networks in FTIR spectroscopy. *Spectrosc. Lett.* **1999**, *32* (3), 421–429.
21. Liu, P.; Liang, Y. Z.; Wang, S. G.; Song, X. H.; Yu, R. Q. Artificial neural networks for non-line multivariate calibration of fluorescence spectra. *Acta Chim. Sinica* **1997**, *54*, 386–392.
22. Phelan, M. K.; Barlow, C. H.; Kelty, J. J.; Jinguji, T. M.; Callis, J. B. Measurement of caustic and caustic brine solutions by spectroscopic detection of the hydroxideion in the near infrared region 700–1150 nm. *Anal. Chem.* **1989**, *61*, 1419–1424.
23. Carey, W. P.; Wangen, L. E. Spectrophotometric method for the analysis of plutonium and nitric acid using partial least squares regression. *Anal. Chem.* **1989**, *61*, 1667–1669.
24. Zupan, J.; Gasteiger, J. Neural networks: a new method for solving chemical problems or just a passing phase? *Anal. Chim. Acta* **1991**, *248*, 1–30.
25. Anker, L. S.; Jurs, P. C. Prediction of carbon-13 nuclear magnetic resonance chemical shifts by artificial neural networks. *Anal. Chem.* **1992**, *64*, 1157–1164.
26. Burns, J. A.; Whitesides, G. M. Feed-forward neural networks in chemistry: mathematical systems for classification and pattern recognition. *Chem. Rev.* **1993**, *93* (8), 2583–2601.
27. Li, Y.; Wang, J. D.; Yuan, W. Q. Simulraneous determination and spectra correction of air toxic organic compounds using PLS and ANN in FTIR spectroscopy. *J. Environ. Sci. Health A* **2000**, *A35* (9), 1673–1691.
28. Tang, A. Q.; Yang, Z. Z.; Ye, Y. J. The transformation rule of homologues' character and the terminal group effect. In *Quantum Chemistry of Macromolecular System*; Jilin University Press: Changchun, 2000; pp. 92–93.